

Fabrication of TiO₂ Nanofibers from a Mesoporous Silica Film

Chunrong Xiong and Kenneth J. Balkus, Jr.*

Department of Chemistry and the UTD Nanotech Institute, The University of Texas at Dallas,
Richardson, Texas 75083-0688

Received April 18, 2005. Revised Manuscript Received May 18, 2005

TiO₂ nanofibers have been made by impregnating a mesoporous silica film with TiCl₄ followed by hydrolysis in air. The TiO₂ nanofiber morphology can be varied by controlling the pore size and pore volume of the mesoporous silica film. TiO₂ nanofiber diameters were in the range of 30–200 nm. The as-synthesized nanofibers are amorphous but crystallize to anatase at 250 °C without a change in morphology.

Introduction

Nanostructured TiO₂ films have attracted attention for a great variety of applications, such as dye-sensitized solar cells,^{1,2} photocatalysis,^{3–6} various cleaning devices,^{7–9} and antifog windows.^{10–12} A number of techniques have been used to make TiO₂ films, including evaporation,^{13,14} sputtering,^{15,16} sol–gel,^{17,27} chemical vapor deposition (CVD),^{18–25} plasma-enhanced chemical vapor deposition,²⁶ and pulsed

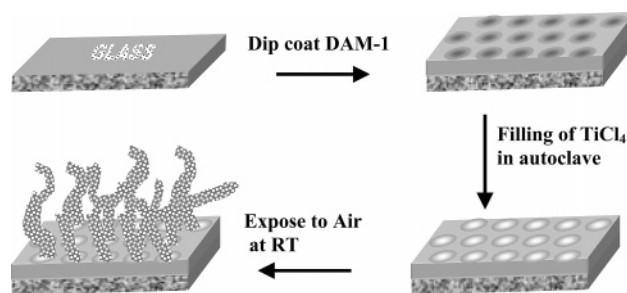


Figure 1. Scheme for the formation of TiO₂ nanofibers from mesoporous silica films.

* Corresponding author. Tel: 972-883-2659. Fax: 972-883-2925. E-mail: balkus@utdallas.edu.

- (1) Nazeeruddin, M. K.; Kay, A.; Rodico, I.; Humphry-Baker, R.; Liska, P. Vlachopoulos, N.; Grätzel, M. *J. Am. Chem. Soc.* **1993**, *115*, 6382.
- (2) O'Regan, B.; Grätzel, M. *Nature* **1991**, *353*, 737.
- (3) Lachheb, H.; Puzeat, F.; Houas, A.; Ksibi, M.; Elaloui, F.; Guillard, C.; Herrmann, J. M. *Appl. Catal., B* **2002**, *39*, 75.
- (4) Linsebrügler, A. L.; Lu, G.; Yates, J. T. *Chem. Rev.* **1995**, *95*, 735.
- (5) Tanguay, J. F.; Suib, S. L.; Coughlin, R. W. *J. Catal.* **1989**, *17*, 335.
- (6) Sivalingam, G.; Nagaveni, K.; Hegde, M. S.; Madras, G. *Appl. Catal. B: Environ.* **2003**, *45*, 23.
- (7) Joannopoulos, J. D.; Villeneuve, P. R.; Fan, S. *Nature* **1997**, *386*, 143.
- (8) Sunada, K.; Kikuchi, Y.; Hashimoto, K.; Fujishima, A. *Environ. Sci. Technol.* **1998**, *32*, 726.
- (9) Cai, R.; Kubota, Y.; Shuin, T.; Hashimoto, K.; Fujishima, A. *Canc. Res.* **1992**, *52*, 2346.
- (10) Wang, R.; Hashimoto, K.; Fujishima, A.; Chikuni, M.; Kojima, E.; Kitamura, A.; Shimohigoshi, M.; Watanabe, T. *Nature* **1997**, *388*, 431.
- (11) Wang, R.; Hashimoto, K.; Fujishima, A.; Chikuni, M.; Kojima, E.; Kitamura, A.; Shimohigoshi, M. *Adv. Mater.* **1998**, *10*, 135.
- (12) Wang, R.; Sakai, N.; Fujishima, A.; Watanabe, T.; Hashimoto, K. *J. Phys. Chem. B* **1999**, *103*, 2188.
- (13) Brown, W. D.; Grannemann, W. W. *Solid-State Electron.* **1978**, *21*, 837.
- (14) Grosslaux, W.; Unshan, R. F. B. *J. Vac. Sci. Technol.* **1975**, *12*, 593.
- (15) Schiller, S.; Beister, G.; Sieber, W.; Schirmer, G.; Hacker, E. *Thin Solid Film* **1981**, *83*, 239.
- (16) Suhail, M. H.; Mohan Rao, G.; Mohan, S. *J. Appl. Phys.* **1992**, *71*, 1421.
- (17) Yoko, T.; Yuasa, A.; Kamiya, K.; Sakka, S. *J. Electrochem. Soc.* **1991**, *138*, 2279.
- (18) Yeung, K. S.; Lam, Y. W. *Thin Solid Films* **1983**, *109*, 169.
- (19) Fuyuki, T.; Matsunami, H. *Jpn. J. Appl. Phys.* **1986**, *25*, 1288.
- (20) Williams, L. M.; Hess, D. W. *J. Vac. Sci. Technol. A* **1983**, *1*, 1810.
- (21) Chen, Z. X.; Derking, A. *J. Mater. Chem.* **1993**, *11*, 1137.
- (22) Fictorie, C. P.; Evans, J. F.; Gladfelter, W. L. *J. Vac. Sci. Technol. A* **1994**, *12*, 1108.
- (23) Lu, J. P.; Raj, R. *J. Mater. Res.* **1991**, *6*, 1913.
- (24) Siefert, K. L.; Griffin, G. L. *J. Electrochem. Soc.* **1990**, *137*, 814.
- (25) Frenc, H. J.; Wulisch, W.; Kuhr, M.; Kassing, R. *Thin Solid Films* **1991**, *201*, 327.
- (26) Huang, S. S.; Chen, J. S. *J. Mater. Sci: Mater. Electron* **2002**, *13*, 77.
- (27) Miki, T.; Nishizawa, K.; Suzuki, K.; Kato, K. *Mater. Lett.* **2004**, *58*, 2751.

laser deposition.²⁸ It is known that many of these applications would benefit from high surface to volume particles. For example, the maximum photoconversion efficiency for water splitting has been increased by more than 2-fold through replacing TiO₂ nanocrystalline films with TiO₂ nanowires.²⁹

Recently, Wu and Yu³⁰ synthesized TiO₂ nanorods using metal-organic chemical vapor deposition (MOCVD). Peng and Chen³¹ fabricated rutile TiO₂ nanorod arrays by oxidizing titanium metal with acetone as the oxygen source. Weng et al.³² reported the synthesis of needlelike rutile TiO₂ nanostructures on a silica substrate containing TiO₂ seeds prepared through a thin PS-*b*-P4VP diblock copolymer template. TiO₂ nanotubes and fibers have also been prepared under hydrothermal conditions³³ as well as by treatment of a dense film with H₂ at 700 °C.³⁴ Miao et al.³⁵ prepared anatase TiO₂ nanowires within the pores of an anodic aluminum oxide (AAO) template by a cathodically induced sol–gel method. In this case, formation of TiO₂ nanofibers takes place inside the pores but access to the fibers requires dissolution of the AAO template.

- (28) Usui, H.; Miyamoto, O.; Nomiya, T.; Horie, Y.; Miyazaki, T. *Sol. Energy Mater. Sol. Cells* **2005**, *86*, 123.
- (29) Khan, S. U. M.; Sultana, T. *Sol. Energy Mater. Sol. Cells* **2003**, *76*, 211.
- (30) Wu, J. J.; Yu, C. C. *J. Phys. Chem. B* **2004**, *108*, 3377.
- (31) Peng, X.; Chen, A. *J. Mater. Chem.* **2004**, *14*, 2542.
- (32) Weng, C. C.; Hsu, K. F.; Wei, K. H. *Chem. Mater.* **2004**, *16*, 4080.
- (33) Yuan, Z. Y.; Su, B. L. *Colloids Surf. A* **2004**, *241*, 173.
- (34) Yoo, S.; Akbar, S. A.; Sandhage, K. H. *Ceram. Int.* **2004**, *30*, 1121.
- (35) Miao, Z.; Xu, D.; Ouyang, J.; Guo, G.; Zhao, X.; Tang, Y. *Nano Lett.* **2002**, *2*, 717.

Table 1. Preparation Conditions and Physiochemical Properties of the Mesoporous Silica Films and TiO₂ Nanofibers^a

samples	mesoporous materials	BET surface areas (m ² /g)	pore volume (cm ³ /g)	pore size (Å)	wall thickness (Å)	thickness of silica layer (μm)	diameter of TiO ₂ fibers (nm)
film A	b	444	0.21	26.5	24.3	0.94	50
film B	c					1.03	no fibers
film C	bare glass						no fibers
film D	d	605	0.42	37.8	28.2	1.08	200
film E	e	1075	0.53	17.0	69.2	1.34	30
film F	f	739	0.56	38.0	99.8	1.41	100

^a For films A, B, C, and D, they were calcined at 400 °C. ^b A gel with a recipe of 0.25 g of Vit E + 35 mL of EtOH + 2.5 mL of 1 M HCl + 1 g of TEOS. ^c Without calcination after being casted the same silica gel as film A. ^d A gel with a recipe of 0.45 g of Vit E + 35 mL of EtOH + 2 mL of 1 M HCl + 1 g of TEOS. ^e A gel with a recipe of 0.2 g of P123 + 0.15 g of CTAB + 5 mL of EtOH + 1.5 mL of 4 M HCl + 1 g of TEOS. ^f A gel with a recipe of 0.35 g of P123 + 5 mL of EtOH + 1.5 mL of 2 M HCl + 1 g of TEOS.

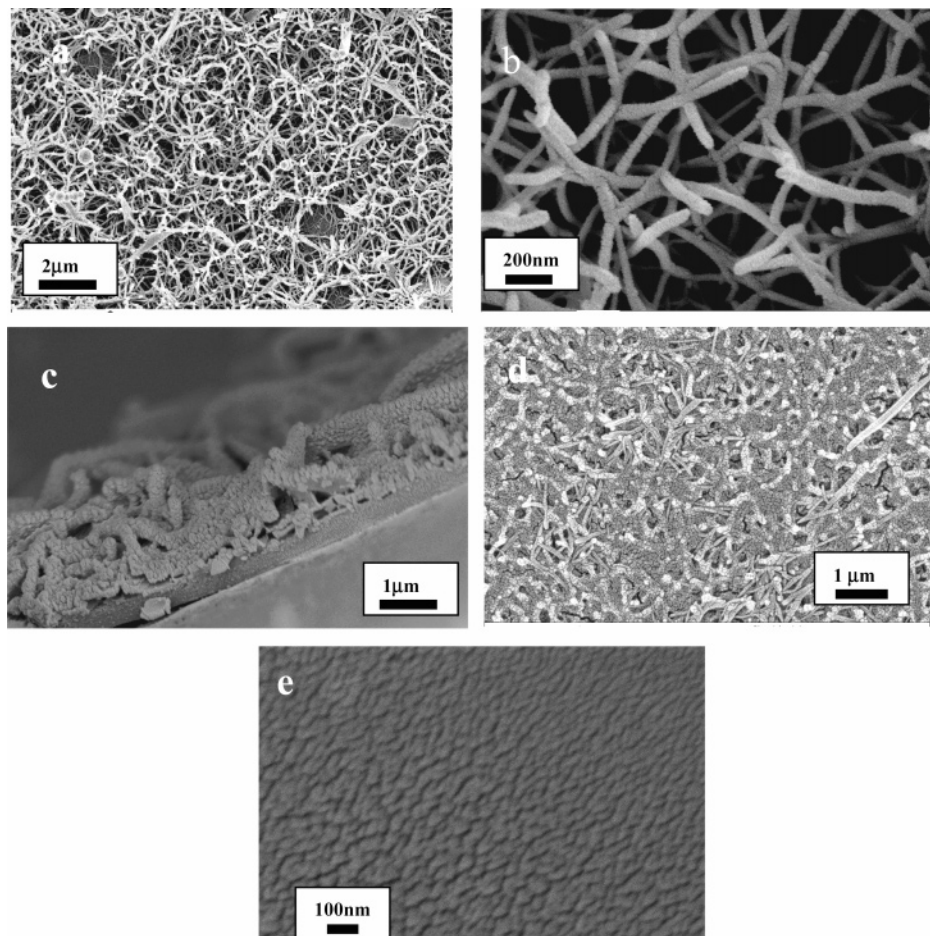


Figure 2. SEM images (a) and (b) are top views of film A, and image (c) is a cross section of film A; image (d) is film C and image (e) is film D after heating at 400 °C.

The confined channels of mesoporous silica powder or silica films have been used to prepare nanoscale metals and metal oxides.^{36–41} In these studies, one common characteristic is that all the desired products formed inside the mesopores of the silica powders or films. Recovery of the nanoparticles

in the pores also requires dissolution of the silica framework which could partially dissolve the encapsulated species. In the present work, a mesoporous silica film was employed as a template to grow TiO₂ nanofibers. This was accomplished by filling the mesopores with TiCl₄ under pressure followed by hydrolysis. The TiCl₄ diffuses out of the pores, making nanofibers 30–150 nm in diameter. The fibers are not formed on the bare glass substrate or on the silica film with the mesopores stuffed with organic template, which is consistent with the role of the mesopores in growing the nanofibers. Additionally, the mesopore diameter has an effect on the diameter of the TiO₂ nanofibers which is also consistent with the template role of the silica film.

- (36) Omer, D.; Ivana, S.; Neil, C.; Geoffrey, A. O. *Adv. Funct. Mater.* **2003**, *13*, 30.
 (37) Atsushi, F.; Hidenobu, A.; Yoko; Yusuke, A.; Masaru, I. *Nano Lett.* **2002**, *2*, 793.
 (38) Shin, H. J.; Ryoo, R.; Liu, Z.; Terasaki, O. *J. Am. Chem. Soc.* **2001**, *123*, 1246.
 (39) Coleman, N. R. B.; Morris, M. A.; Spalding, T. R.; Holmes, J. D. *J. Am. Chem. Soc.* **2001**, *123*, 187.
 (40) Gao, F.; Lu, Q.; Zhao, D. Y. *Adv. Mater.* **2003**, *15*, 739.
 (41) Han, Y. J.; Kim, J. M.; Stucky, G. D. *Chem. Mater.* **2000**, *12*, 2068.

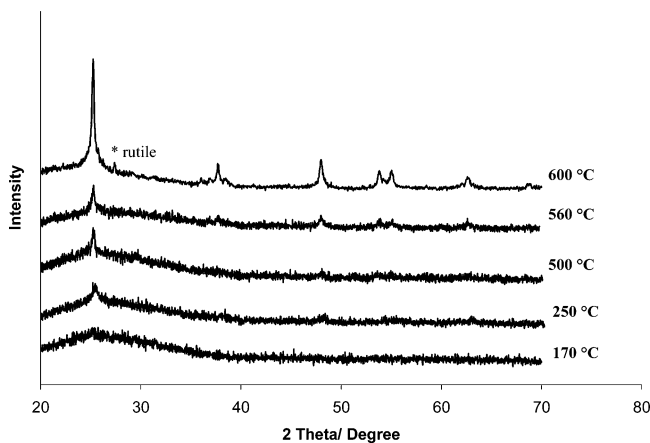


Figure 3. XRD patterns of TiO₂ nanofibers growing on film A after heating at 170, 250, 500, 560, and 600 °C.

Experimental Section

2.1. Materials. Tetraethoxysilane (TEOS, Aldrich), hydrochloric acid (Mallinckrodt), vitamin E TPGS (Eastman), ethyl alcohol (Aldrich), Pluronic P123 (BASF), cetyltrimethylammonium bromide (CTAB, Aldrich), and TiCl₄ (Chemat technology, Inc.) were used as received.

2.2. Preparation of Mesoporous Silica Films. The precursor for the casting sol solution is prepared from two solutions. One is a template solution, containing the template dissolved in ethanol (EtOH). The other is a silica solution, which contains a mixture of tetraethyl orthosilicate (TEOS), EtOH, distilled water, and hydrochloric acid. The specific recipes are listed in Table 1. These template and silica solutions are mixed and then condensed by partially evaporating EtOH at room temperature. The gel is then cast onto glass slides, dried at room temperature for 5 h, and calcined at 400 °C for 10 h.

2.3. Preparation of TiO₂ Nanofiber Films. Glass slides covered with the mesoporous silica film were placed in a 120 mesh stainless steel screen basket which was positioned in a 23 mL Teflon-lined autoclave 4 cm above 4 mL of TiCl₄. The filling of TiCl₄ in mesopores was conducted by heating the autoclave at 90 °C for 24 h under autogenous pressure. The films were then removed from the autoclave and hydrolyzed in air for 10 min at room temperature with 50% humidity and then dried at 90 °C followed by calcination at 400 °C. For comparison, the same experiment was conducted on the glass slides coated with mesoporous silica but without removal of the organic template. The experiment was also conducted on bare glass slides.

2.4. Characterization. The crystallinity of the TiO₂ nanofibers was determined by powder X-ray diffraction (XRD) (Scintag XDS 2000 X-ray diffractometer with Cu K α radiation). The fiber morphology was evaluated by scanning electron microscopy (LEO 1530 VP field emission SEM) from Au/Pd coated samples. Surface

area and pore size were measured using a Quantachrome Autosorb I, from N₂ absorption and BJH analysis.

Results and Discussion

Four mesoporous silica films to be used as templates were made using Vitamin E TPGS and P123 as well as P123 and CTAB as listed in Table 1. The XRD patterns of these films (not shown) revealed ordered mesoporous structures. The pore sizes of these silica films are also listed in Table 1. To make TiO₂ nanofibers, the mesoporous silica films were subjected to TiCl₄ vapor in an autoclave at 90 °C for 24 h, and then exposed to air for hydrolysis, as illustrated in Figure 1. It was thought that TiO₂ might form in the pores but surprisingly the volatile TiCl₄ vaporizes from pores and reacts with moisture outside the pores of the silica film; thus, TiO₂ nanofibers form on the silica surface.

For the sample film A, Vitamin E TPGS was used as the template to create a 0.94 μm thick DAM-1⁴² film with mesopores 2.65 nm in diameter. Upon filling the sample film with TiCl₄ and after hydrolysis in air, Figure 2a shows a film composed of TiO₂ nanofibers covering the surface of the silica film. The TiO₂ nanofibers have a diameter of \sim 50 nm as displayed in the SEM image in Figure 2b. The TiO₂ nanofibers are larger than the mesopores after complete hydrolysis. It is speculated that the TiCl₄ begins to diffuse out of the pores and begins to hydrolyze, nucleating TiO₂ at the pore opening and/or surface space between pores. The escaping TiCl₄ feeds the growing fiber and eventually more than one fiber merges to form the 50 nm size fibers. The XRD patterns in Figure 3 indicate that as-made TiO₂ nanofibers are amorphous. However, with heating the anatase phase begins to form as low as 250 °C, and the particle size is \sim 50 nm as calculated from the XRD pattern using the Scherrer equation. The anatase phase begins to convert to rutile at 600 °C; meanwhile, the particle size increased to \sim 58 nm.

As a control experiment (film B), a mesoporous silica film containing the Vitamin E TPGS template was treated with TiCl₄ in the same way as film A, but after exposure to air, a film with what appears to be embedded TiO₂ nanorods were observed on the surface (Figure 2d). With the mesopores partially filled with Vitamin E TPGS, the TiCl₄ should mainly adsorb on the outer surface and defect sites. Meanwhile, there are no TiO₂ fibers grown on the bare glass slides (Figure 2e), which further demonstrates the importance of the mesopores for formation of TiO₂ nanofibers on the silica films.

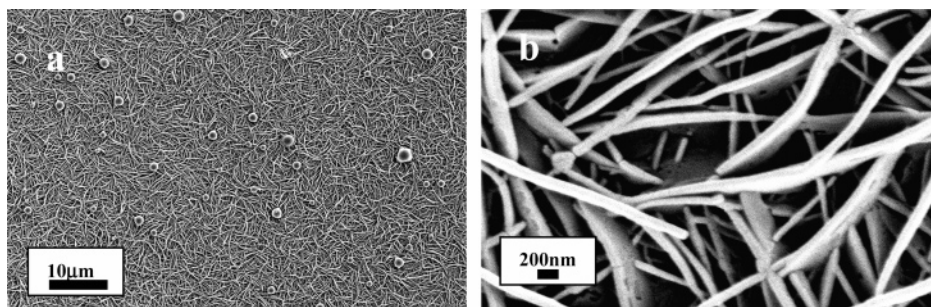


Figure 4. SEM images of film B after heating at 400 °C.

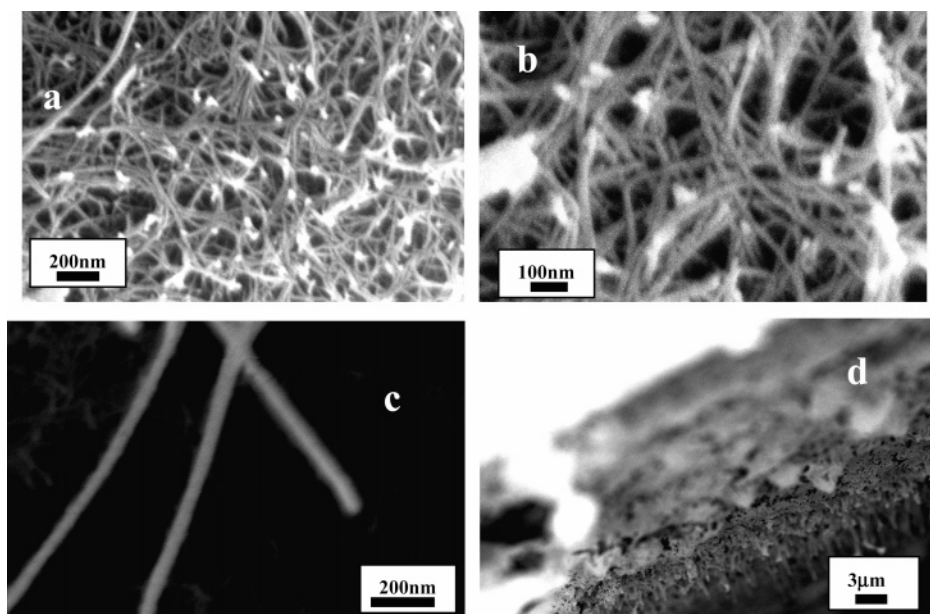


Figure 5. SEM images of film E after heating at 400 °C, where images (a)–(c) are top views and image (d) is a cross section.

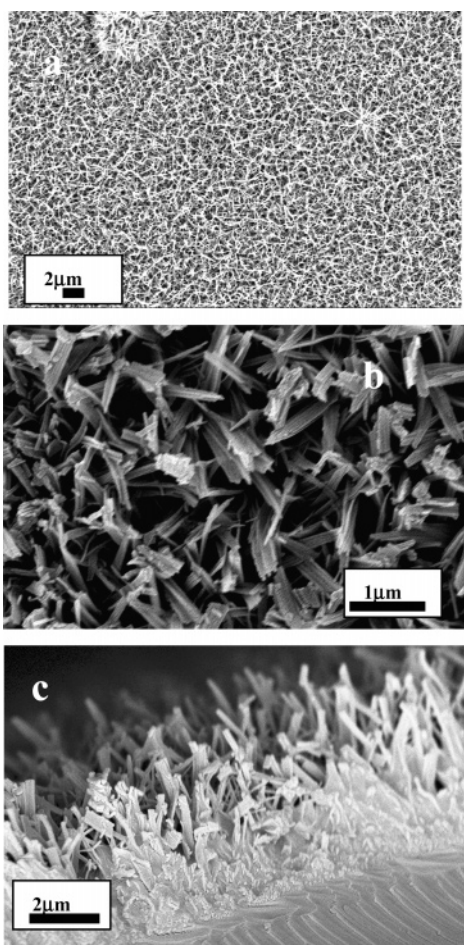


Figure 6. SEM images of film F after heating at 400 °C, where images (a) and (b) are top views and image (c) is a cross section.

When the amount of Vitamin E TPGS was changed in the DAM-1 recipe, film D was prepared with bigger pores (3.78 nm) and pore volume (0.42 cm³/g) in the silica film. Additionally, the mesoporous film is more ordered than film

A (50 nm). After impregnation with TiCl₄ and after hydrolysis, the resulting TiO₂ morphology was ribbon-like as shown in Figure 4. The TiO₂ ribbons formed on the surface of the silica film, with a diameter of 200 nm, which is much bigger than those grown on film A. The increased diameter of TiO₂ may be a result of the bigger pore size in film D; in addition, the bigger pore volume may allow more TiCl₄ to be filled into the film, which may lead to thicker TiO₂ fibers.

To further investigate the effects of pore size and pore volume on the formation of TiO₂ nanofibers, a mesoporous silica film E with a pore size of 1.7 nm was created by using P123 and CTAB as co-templates. For film E, uniform TiO₂ nanofibers exhibited a diameter of ~30 nm as shown in Figure 5c. When P123 was used by itself to prepare film F, the pore size and pore volume of the silica film were increased to 3.8 nm and 0.56 cm³/g, respectively (as seen in Table 1), which is less than usual, because the pore size changes with reaction temperature and time.⁴³ In this case, the mesoporous silica film was made at room temperature, and the reaction time of the precursor before making the silica film was about 3 h. On the surface of film F, larger TiO₂ nanofibers were produced and the diameter was ~100 nm which is consistent with the bigger pore size and the bigger pore volume. The SEM image in Figure 6b suggests the TiO₂ nanofibers are composed of many nanofibers fused together.

Conclusion

A novel mesh of TiO₂ nanofibers has been prepared by filling a mesoporous silica film with TiCl₄ at 90 °C, followed by hydrolysis in air. The size and morphologies of nanofibers appear to change with the pore size and pore volume of the silica layer. XRD patterns of the TiO₂ films indicate the TiO₂ is largely amorphous as made but crystallizes to anatase above 250 °C.

(42) Coutinho, D.; Balkus, K. J., Jr. *Microporous Mesoporous Mater.* **2002**, *54*, 229.

(43) Zhao, D. Y.; Feng, J. L.; Huo, Q.; Melosh, N.; Frederickson, G. H.; Chmelka, B. F.; Stucky, G. D. *Science* **1998**, *279*, 548.

Acknowledgment. We thank the Robert A. Welch foundation for financial support. We also thank Minedys Macias-Guzman and Decio Coutinho for helpful discussions.

Supporting Information Available: XRD patterns of mesoporous silica films. This material is available free of charge via the Internet at <http://pubs.acs.org>.

CM050819H